

MATHEMATICAL MODELING IN ELECTROSPINNING PROCESS OF NANOFIBERS: A DETAILED REVIEW

S. RAFIEI, S. MAGHSOODLOO, B. NOROOZI, V. MOTTAGHITALAB and A. K. HAGHI

University of Guilan, Rasht, Iran

Received July 12, 2012

Electrospinning represents an efficient and versatile technique for fabrication of very thin fibers from polymers or composites. Various polymers have been successfully electrospun into ultrafine fibers in recent years mostly in solvent solution and some in melt form. The efficiency of this process can be improved by adjusting the composition of the solution and the configuration of the electrospinning apparatus, such as voltage, flow rate etc., therefore optimizing the alignment and morphology of the fibers produced. In addition, several applications demand well-oriented and diameter and porosity controlled nanofibers. Thus, recently there has been great interest to optimize this method in order to solve the problems that make electrospinning uncontrollable. Mathematical and theoretical modeling and simulating procedure will permit to offer an in-depth insight into the physical understanding of complex phenomena during electrospinning and might be very useful for managing contributing factors toward increasing production rate. In this review article, we give a general outlook of the most common mathematical models for electrospinning, which have been introduced so far, and briefly point out their weak points.

Keywords: electrospinning, nanofibers, jet instability, modeling

INTRODUCTION

Electrospinning is a simple and relatively inexpensive means of manufacturing high volumes of very thin fibers (typically of 100 nm to 1 micron), with lengths up to kilometers, from a vast variety of materials, including polymers, composites and ceramics.¹⁻² Electrospinning technology was first developed and patented by Formhals³ in the 1930s, and a few years later the actual developments were triggered by Reneker and co-workers.⁴ These techniques have been investigated and developed to satisfy the increasing needs for the refined nanosize hybrid fibers based on commercial polymers.⁵ Electrospinning has proven to be the best nanofiber manufacturing process due to simplicity and material compatibility.⁶ A survey of open publications related to electrospinning in the past decade is given in Figure 1.

In this method, nanofibers are produced by solidification of a polymer solution stretched by an

electric field.⁷⁻⁹ The unique properties of nanofibers are extraordinarily high surface area per unit mass, very high porosity, tunable pore size and surface properties, layer thinness, high permeability, low basic weight, ability to retain electrostatic charges and cost effectiveness.² These electrospun nanofibers can be applied in different areas, including wound dressing, drug or gene delivery vehicles, biosensors, fuel cell membranes and electronics, tissue-engineering processes. Table 1 illustrates the percentage of studies devoted to different applications of electrospun nanofibers in various industries, as reported in literature.^{8,10-11}

There are commonly two standard electrospinning setups, vertical and horizontal. By developing this technology, several researchers have developed more intricate systems that can fabricate more complex nanofibrous structures in a more controlled and efficient style.¹¹

As Figure 2 shows, during the electrospinning procedure, a polymer solution or melt is supplied through a syringe about 10-20 cm above a grounded substrate. The process is driven by an electrical potential, which is applied between the syringe and the substrate.¹⁰ Electrospinning of polymer solutions involves, to a first approximation, a rapid evaporation of the solvent. The evaporation of the

solvent thus will happen on a time scale well below the second-range.¹² The elongation of the jet during electrospinning is initiated by electrostatic force, gravity, inertia, viscosity and surface tension.¹ Unlike the traditional spinning process, which principally uses gravity and externally applied tension, electrospinning uses externally applied electric field, as driving force.⁵⁻⁶

Table 1
Application of electrospun polymer nanofibers

Application of polymer nanofibers	Percents (%)
Tissue engineering	70
Nano-sensors	10
Industrial application	8.4
Filter media	5
Protective clothing	4.3
Life science	1.3
Cosmetics	1

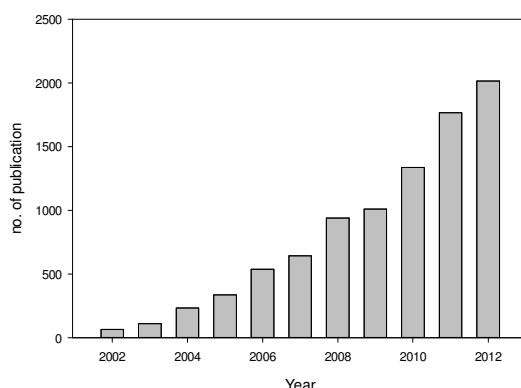


Figure 1: Diagram of electrospinning publications in last decade

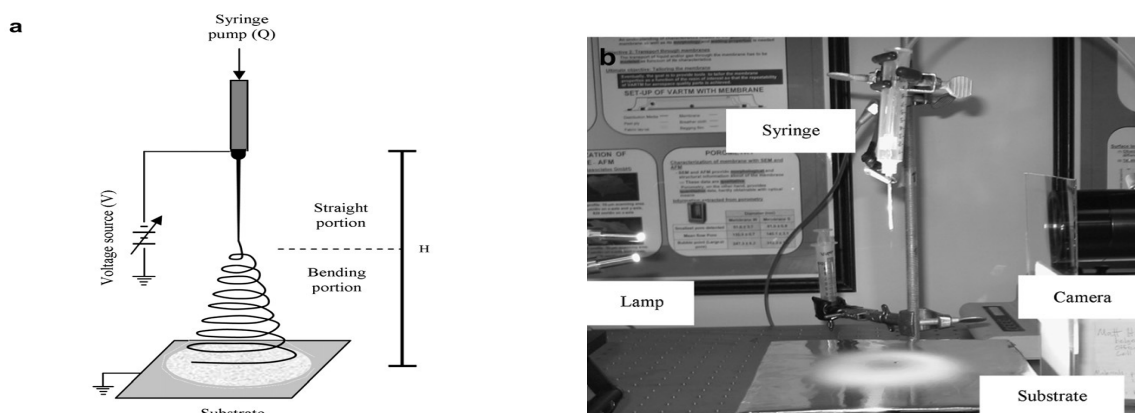


Figure 2: Electrospinning set-up for nanofiber production¹⁰

The applied voltage induces a high electric charge on the surface of the solution drop at the needle tip. The drop now experiences two major electrostatic forces: the Coulombic force, which is induced by the electrical field, and the electrostatic repulsion between the surface charges. The intensity of these forces causes the hemispherical surface of the drop to elongate and form a conical shape, which is also known as the Taylor cone. By further increasing the strength of the field, the electrostatic forces in the drop will overcome the surface tension of the fluid/air interface and an electrically charged jet will be ejected.¹³ As the jet diameter decreases, the surface charge density increases and the resulting high repulsive forces split the jet into smaller jets. This phenomenon may occur several times, leading to many small jets.¹⁴ After the ejection, the jet elongates and the solvent evaporates, leaving an electrically charged fiber which, during the elongation process, becomes very thin.^{1-2,12,15}

The characteristic feature of this process is the onset of a chaotic oscillation of the elongating jet, which is due to the electrostatic interactions between the external electric field and the surface charges on the jet, as well as the electrostatic repulsion of mutual fiber parts. The fiber can be spun directly onto the grounded (conducting) screen or on an intermediate deposit material. Because of the oscillation, the fiber is deposited randomly on the collector, creating a so-called “non-woven” fiber fabric.^{1,16}

Recent experiments demonstrate that an essential mechanism of electrospinning is a rapidly whipping fluid jet. These studies analyze the mechanics of this whipping jet by studying the instability of an electrically forced fluid jet with increasing field strength. Generally, three different instabilities are identified: the classical (axisymmetric) Rayleigh instability and electric field induced axisymmetric and whipping instabilities. By increasing field strengths, the electrical instabilities are enhanced, whereas the Rayleigh instability is suppressed. Which instability dominates depends strongly on the surface charge density and radius of the jet.¹⁶⁻¹⁷ These instabilities depend on fluid parameters and equipment configuration such as location of electrodes and the form of spinneret.¹⁶

In melt or dry/wet solution spinning, the shape and diameter of the die, as well as the mechanical forces inducing specific draw ratios and drawing speeds highly determine dimensional and structural properties of the final fibers.¹⁸ But in electrospinning, the effective properties known are the polymer molecular weight, the molecular weight distribution, the architecture (branched, linear etc.) of the polymer, temperature and humidity and air velocity in the chamber and processing parameters (like applied voltage, flow rate, types of collectors, tip to collector distance) as well as the rheological and electrical properties of the solution (viscosity, conductivity, surface tension etc.) and finally motion of target screen.^{2,8,11,19} The processing parameters mentioned above can be manipulated so that a steady, electrostatically driven jet of fluid is drawn from the capillary tip and is collected upon the grounded substrate.^{2,10,16} Studying the effects of various electrospinning parameters is important to improve the rate of nanofiber processing. In addition, several applications demand well-oriented nanofibers.⁶ Several techniques, such as dry rotary electrospinning²⁰ and scanned electrospinning nanofiber deposition system,²¹ control the deposition of oriented nanofibers.

Fiber diameter is the most important structural characteristic in electrospun nanofiber webs. Despite the importance, there is no successful method for determining fiber diameter yet, although a few studies have been conducted to develop a method for measuring it.²² Fiber diameter is usually determined from Scanning Electron Microscopy (SEM) images obtained of the electrospun webs. Because of the small fiber dimensions, high-quality images with appropriate magnifications are required. Another tried method for nanofiber diameter measuring is applying an image analysis based on a binary image of the textile. It is used to create a distance map and skeleton. The fiber diameter may be determined from the values of the distance map at any pixel location on the skeleton.²²⁻²³ The other common ways are transmission electron microscopy (TEM) and atomic force microscopy (AFM).²² RSM (response surface methodology) has also been successfully used for process optimization and obtaining a quantitative relationship between electrospinning

parameters and the average fiber diameter and its distribution.²⁴⁻²⁵ Artificial neural networks (ANN) also have been successfully applied for modeling and controlling the electrospinning processes in recent years. ANN cannot create an equation similar to RSM, but it works as human brain does and it estimates the response based on the trained data in the inquired range.^{22,24,26} Rabbi *et al.*²⁷ have employed RSM and ANN methods to analyze polyurethane (PU) and polyacrylonitrile (PAN) nanofiber morphology, synthesized by electrospinning in order to determine the parameters that may affect the nanofibers morphology and optimize the process.^{25,27} Porosity is another important property of electrospun webs, which can be measured by using SEM, TEM and FEM image analysis.²⁸

Studies by Frenot *et al.*¹⁹ indicated some important findings and namely that: (i) fibers of different sizes, i.e. consisting of different numbers of parent chains, exhibit almost identical hyperbolic density profiles at the surfaces, (ii) the end beads are predominant and the middle beads are depleted at the free surfaces, (iii) there is an anisotropy in the orientation of bonds and chains at the surface, (iv) the centre of mass distribution of the chains exhibits oscillatory behavior across the fibers and (v) the mobility of the chain in nanofiber increases as the diameter of the nanofiber decreases.

An important weak point of the electrospinning method is a convective instability in the elongating jet. The jet will start rapidly whipping as it travels

towards the collector. Therefore, during the electrospinning process, the whole substrate is covered with a layer of randomly placed fiber. The created fabric has a chaotic structure and it is difficult to characterize its properties.^{1,6} Another weak point is that electrospun fibers often have beads as “by-products”.²⁹ Some polymer solutions are not easily electrospun when the polymer solution is too dilute, due to limited solubility of the polymer. In these cases, the lack of elasticity of the solution prevents the formation of uniform fibers; instead, droplets or necklace-like structures known as “beads-on-string” are formed.³⁰ The electrospun beaded fibers are related to the instability of the jet of the polymer solution. The bead diameter and spacing are related to fiber diameter, solution viscosity, net charge density carried by the electrospinning jet and surface tension of the solution.²⁹⁻³⁰

A striking feature of the electrospinning process is that jets can be launched, in principle, from any liquid surface. Thus, a variety of configurations have been reported that produce jets from free liquid surfaces without the use of a spinneret. These contain the use of a magnetic liquid in which “spikes” can be formed to concentrate field lines at points on a liquid surface, liquid-filled trenches, wetted spheres, cylinders and disks, conical wires, rotating beaded wires and gas bubbles rising through the liquid surface.³¹ One of the perceived drawbacks of electrospinning for industrial purposes is its low production rate.

Table 2
Comparison of nozzle vs. nozzle-less electrospinning

Production variable	Nozzle	Nozzle-less
Mechanism	Needle forces polymer downwards Drips and issues deposited in web	Polymer is held in bath; even distribution is maintained on electrode via rotation
Hydrostatic pressure	Production variable – required to be kept level across all needles in process	None
Voltage	5-20 kV	30-120 kV
Taylor cone separation	Defined mechanically by needle distance	Nature self-optimizes distance between Taylor cones
Polymer concentration	Often 10% of solution	Often 20% or higher of solution
Fiber diameters	80, 100, 150, 200, 250 and higher Standard deviation likely to vary over fiber length	80, 100, 150, 200, 250 and higher Standard deviation of $\pm 30\%$

The nozzle-less (free liquid surface) technology create possibilities to produce nanofiber layers at a mass industrial scale. Nanofiber non-woven structured layers are ideal for creating composite materials.²⁰

Generally, a model is a schematic description of a system, theory, or phenomenon that accounts for its known or inferred properties and may be used for further study of its characteristics. A mathematical modeling is a representation in mathematical terms of the behavior of real devices and objects. Since the modeling of devices and phenomena is essential to both engineering and science, engineers and scientists have very practical reasons for doing mathematical modeling. In this way, models are classified into three groups, models that describe the behavior or results observed, models that explain why that behavior and results occurred as they did, and models that allow us to predict future behaviors or results that are as yet unseen or unmeasured.

Despite the simplicity of the electrospinning technology, industrial applications of electrospinning are still relatively rare, mainly due to the unresolved problem of very low fiber throughput for existing devices and difficulties in controlling the process. Collection of experimental data and their confrontation with simple physical models appears as an effective approach towards the development of practical tools for controlling and optimizing the electrospinning process.³² On the other hand, it is necessary to develop theoretical and numerical models of electrospinning because of demands for different optimization procedures for each material.⁸ Utilizing a model to express the effect of electrospinning parameters will assist researchers in presenting in an easy and systematic way the influence of variables and thus controlling the process. Additionally, this would help predict the results under a new combination of parameters. Therefore, without conducting any experiments, one can easily estimate features of the product under unknown conditions.³³ In general, modeling and simulation of electrospinning process are useful in understanding the following:

- a) the cause for whipping instability;
- b) the dependence of jet formation and jet instability on the process parameters and fluid

properties, for better jet control and higher production rate;

- c) the effect of secondary external field on jet instability and fiber orientation.^{2,6}

In the following section, some necessary basic theories for electrospinning modeling are reviewed.

THE BASICS OF ELECTROSPINNING MODELING

As was discussed, the modeling of the electrospinning process is valuable for acquiring knowledge on factors that cannot be measured experimentally.³⁴ As mentioned before, although electrospinning gives continuous fibers, mass production and the ability to control nanofiber properties have not been obtained yet. On the other hand, during this procedure, nanofibers gather randomly on the collector plate; while, in applications such as tissue engineering, well-oriented nanofibers are needed. Mathematical and theoretical modeling of the electrospinning process has been attempted by many researchers to solve these problems. Recently, several models and simulations were introduced to present a better understanding of electrospinning jet mechanics.⁶ The development of a relatively simple model of the process was limited by the lack of systematic, fully characterized experimental observations.¹⁶ The governing parameters of the electrospinning process, which are effective on the macroscopic nanofiber properties and commonly investigated by the modeling, are solution volumetric flow rate, polymer weight concentration, molecular weight, the applied voltage and the nozzle to ground distance.^{1,7,35} Polymeric jet ejection is focused on for simulation and modeling more than other parts of the electrospinning process.

As discussed already, by overcoming surface tension, the polymer jet would be ejected from the nozzle. In the first stage, the jet thins until the instability point. In the second stage, the jet becomes unstable and undergoes a whipping process. The jet then leaves behind a thin thread of polymer on the collector. Accordingly, two important modeling zones have been introduced so far, which are: a) the zone close to the capillary (jet initiation zone) outlet of the jet and b) the whipping instability zone, in which the jet spirals and accelerates towards the collector plate.^{6,34,36}

It is necessary to study the parameters that influence the nature and diameter of the final fiber to obtain the ability to control morphology. For selected applications, it is desirable to control not only the fiber diameter, but also the internal morphology.³⁷ An ideal operation is one in which the nanofiber diameter is controllable, the surface of the fibers is intact and a single fiber would be collectable. The control of the fiber diameter can be affected by the solution concentration, the electric field strength, the feeding rate at the needle tip and the gap between the needle and the collecting screen.^{1,12,38}

The concentration of the polymer solution is the most important parameter effective on final nanofiber morphology. Depending on solution concentration during experiments, various impacts for the electric field were observed. Since the

effects of solution concentration and electric field strength on mean fiber diameter change at different spinning distances, some interactions and coupling effects are present between the parameters.³³ Figure 3 presents the effect of process parameters on fiber diameter.

The disadvantages of the electrospinning method, such as low production rate, non-oriented nanofiber production, difficulty in diameter prediction and control of nanofiber morphology, absence of enough information on the rheological behavior of the polymer solution and difficulty in precise process control, emphasize the necessity of modeling. Generally, a suitable theoretical model of the electrospinning process is one which can show strong-moderate-minor rating effects of these effective parameters on fiber morphology.^{35,38-39}

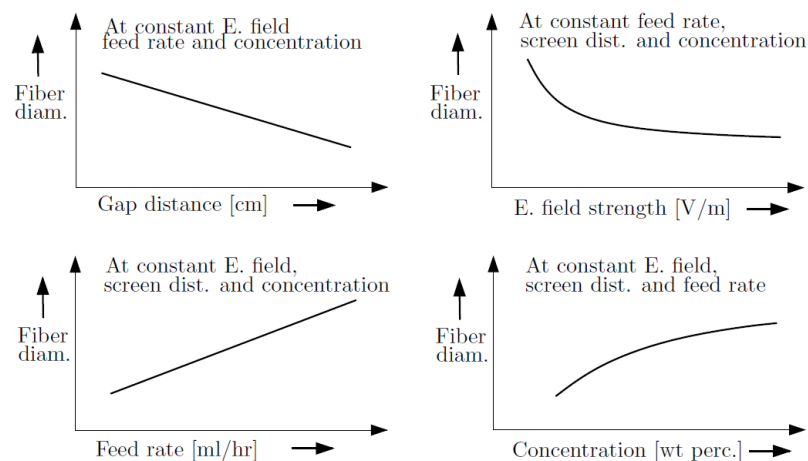


Figure 3: Effect of process parameters on fiber diameter¹

Viscoelastic flow analysis

Understanding the effects of viscoelasticity on the electrospinning process is important due to its relevance in the creation of fibers made from polymers, glasses, and combinations thereof. In spite of this, most researches on modeling are limited to the study of Newtonian fluids, and so do not describe accurately the rheology of viscoelastic materials.

Viscosity plays an important role in determining the rate of jet thinning during jet elongation. Feng *et al.*³⁶ have furthermore extended the slender jet model to include viscoelastic effects, which will be

discussed later. The primary role of extensional thickening is to alter the shape of the jet in the intermediate regime of the thinning jet, resulting in sharply thinning cone-jets. Recent experimental studies of model Boger fluids confirm the rapid initial thinning of the cone-jet, for viscoelastic fluids, and suggest the emergence of a new regime where the scaling of diameter with distance along the jet increases from the inverse 1/4 power, typical of Newtonian fluids, towards the inverse 1/2 power for fluids with strong extensional thickening.⁴⁰

Recently, significant progress has been made in the development of numerical algorithms for the

stable and accurate solution of viscoelastic flow problems, related to methods like electrospinning. There is still a limitation in applying mixed finite element methods to solve viscoelastic flows using constitutive equations of the differential type.⁴¹⁻⁴² Due to the importance of these analyses, some aspects of viscoelastic flow analysis are further mentioned briefly, before discussing about modeling details.

The analysis of viscoelastic flows includes the solution of a coupled set of partial differential equations. The equations commonly depicting the conservation of mass, momentum and energy, and constitutive equations for a number of physical quantities present in the conservation equations, such as density, internal energy, heat flux, stress etc. depend on the process discussed later.⁴¹

The constitutive equation may be transformed into an ordinary differential equation (ODE). For transient problems, this can, for instance, be achieved in a natural manner by adopting a Lagrangian formulation.⁴³ By introducing a selective implicit/explicit treatment of various parts of the equations, a certain separation at each step of the set of equations may be obtained to improve computational efficiency. This suggests the possibility to apply devoted solvers to sub-problems of each fractional time step.⁴¹

Lattice Boltzmann method (LBM)

An efficient numerical modeling for complex structure web with a reliable prediction needs a complete description of the structure, which is highly difficult. One of these models in agreement with experiments is lattice Boltzmann method.⁴⁴ Developing lattice Boltzmann method instead of traditional numerical techniques, like finite volume, finite difference and finite element, for solving large-scale computations and problems involving complex fluids, colloidal suspensions and moving boundaries is very useful.⁶

Basics of hydrodynamics

As nanofibers are made of polymeric solution forming jets, it is necessary to have basic knowledge of fluid hydrodynamics.⁴⁵ In the attempt of finding a fundamental description of fluid dynamics, the theory of continuity was implemented. The theory describes fluids as small elementary volumes (Figure 4), which still consist

of many elementary particles. Some important equations of fluid hydrodynamics due to this theory are presented below:

The equation of continuity:

$$\frac{\partial \rho_m}{\partial t} + \text{div}(\rho_m v) = 0 \quad (\text{For incompressible fluids } \text{div}(v) = 0) \tag{1}$$

Euler’s equation simplified for electrospinning:

$$\frac{\partial v}{\partial t} + \frac{1}{\rho_m} \nabla p = 0 \tag{2}$$

The equation of capillary pressure:

$$P_c = \frac{\gamma \partial^2 \zeta}{\partial x^2} \tag{3}$$

The equation of surface tension:

$$\Delta P = \gamma \left(\frac{1}{R_x} + \frac{1}{R_y} \right) \tag{4}$$

R_x and R_y are radii of curvatures

The equation of viscosity:

$$\tau_{ij} = \eta \left(\frac{\partial v_i}{\partial x_j} + \frac{\partial v_j}{\partial x_i} \right) \tag{5}$$

(For incompressible fluids, τ_{ij} = Stress tensor)

$$V = \frac{\eta}{\rho_m} \tag{6}$$

(Kinematic viscosity)

Electrohydrodynamic (EHD) theory

In 1966, Taylor discovered that finite conductivity enables electrical charge to accumulate at the drop interface, permitting a tangential electric stress to be generated. The tangential electric stress drags fluid into motion, and thereby generates hydrodynamic stress at the drop interface. The complex interaction between the electric and hydrodynamic stresses causes either oblate or prolate drop deformation, and in some special cases keeps the drop from deforming.⁴⁶⁻⁴⁷

Feng¹⁰ used a general treatment of Taylor-Melcher for the stable part of electrospinning jets by one-dimensional equations for mass, charge and momentum. In this model, a cylindrical fluid element is used to show electrospinning jet kinematic measurements.

In Figure 4, the essential parameters are presented: radius, R , velocity, v_z , electric field, E_z , total path length, L , interfacial tension, γ , interfacial charge, σ , tensile stress, τ , volumetric flow rate, Q ,

conductivity, K , density, ρ , dielectric constant, ε , and zero-shear rate viscosity, η_0 . The most important equations that Feng used are the following:^{10,48}

$$\tilde{R}^2 \tilde{v}_z = 1 \tag{7}$$

$$\tilde{R}^2 \tilde{E}_z + Pe_e \tilde{R} \tilde{v}_z \tilde{\sigma} = 1 \tag{8}$$

$$\tilde{v}_z \tilde{v}'_z = \frac{1}{Fr} + \frac{\tilde{T}'}{Re_j \tilde{R}^2} + \frac{1}{We} \frac{\tilde{R}'}{\tilde{R}^2} + \varepsilon (\tilde{\sigma} \tilde{\sigma}' + \beta \tilde{E}_z \tilde{E}'_z + \frac{2\tilde{\sigma} \tilde{E}'_z}{\tilde{R}}) \tag{9}$$

$$\tilde{E}_z = \tilde{E}_0 - \ln \chi \left[(\tilde{\sigma} \tilde{R})' - \frac{\beta}{2} (\tilde{E} \tilde{R}^2)' \right] \tag{10}$$

$$E_0 = \frac{\eta_0 V_0}{R_0} \tag{11}$$

$$\beta = (\varepsilon/\tilde{\varepsilon}) - 1 \quad \tau = R^2 (\tilde{\tau}_{zz} - \tilde{\tau}_{rr})$$

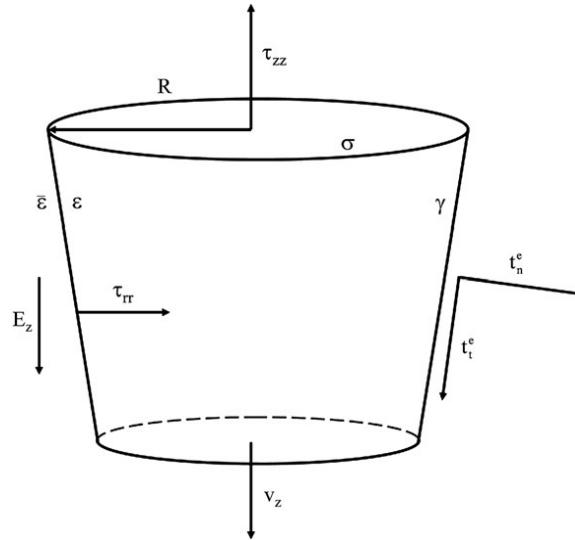


Figure 4: Scheme of the cylindrical fluid element used in electrohydrodynamic modeling¹⁰

Feng solved the equations for different fluid properties, particularly for non-Newtonian fluids with extensional thinning, thickening, and strain hardening, but Helgeson *et al.*¹⁰ developed a simplified understanding of electrospinning jets based on the evolution of the tensile stress due to elongation.

Electric forces in fluids

The initialization of instability on the surfaces of liquids is done by applying the external electric field, inducing electric forces on surfaces of liquids. A localized approximation was developed to calculate the bending electric force which acts on an electrified polymer jet, as an important element of the electrospinning process for manufacturing of nanofibers. Using this force, a far reaching analogy between the electrically driven bending instability and the aerodynamically driven instability was established. The description of the wave's instabilities is expressed by equations called dispersion laws. The dependence of wavelength on

the surface tension is almost linear and the wavelengths between jets are a little bit smaller for lower depths. The dependence of wavelength on electric field strength is exponential. The dispersion law is identified for four groups of dielectric liquids, using Clausius-Mossotti and Onsager's relation (non-polar liquids with finite and infinite depth and weakly polar liquids with finite and infinite depth). According to these relations, relative permittivity is a function of parameters like temperature, square of angular frequency, wavelength number and reflective index.^{2,45,49-50}

Dimensionless non-Newtonian fluid mechanics method

The best way for analyzing fluid mechanics problems is to convert parameters to a dimensionless form. By using this method, the numbers of governing parameters for given geometry and initial condition reduce. The non-dimensionalization of a fluid mechanics problem generally starts with the selection of a characteristic

velocity, then because of the flow of non-Newtonian fluids, the stress depends non-linearly on the flow kinematics, the deformation rate is a main quantity in the analysis of these flows. The next step after determining different parameters is to evaluate characteristic values of the parameters. The non-dimensionalization procedure is to employ the selected characteristic quantities to obtain a dimensionless version of the conservation equations and to get to certain numbers like Reynolds number. The excessive number of governing dimensionless groups poses certain difficulties in the fluid mechanics analysis. Finally, by using these results in the equation and applying boundary conditions, it can be used to study different properties.⁵¹

Detection of X-ray generated by electrospinning

Electrospinning jets, which produce nanofibers from a polymer solution by electrical forces are fine cylindrical electrode creating extremely high electric-field strength in their vicinity under atmospheric conditions. However, this quality of electrospinning is only scarcely investigated, and the interactions of the electric fields generated by them with ambient gases are nearly unknown. Pokorny *et al.*⁵² reported on the discovery that electrospinning jets generate X-ray beaming with energies of up to 20 keV under atmospheric conditions. Mlikes *et al.*⁵³ investigated on the discovery that electrically charged polymeric jets and highly charged gold-coated nanofibrous layers in contact with ambient atmospheric air generate X-ray beams up to energies of hard X-rays.⁵⁴

The first detection of X-ray produced by nanofiber deposition was observed using radiographic films. The main goal of using these films is to understand Taylor cone creation. The X-ray generation is probably dependent on diameters of the nanofibers affected by the flow rate and viscosity. Thus, it is important to find the ideal concentration (viscosity) of polymeric solutions and flow rate to spin nanofibers as thin as possible. The X-ray radiation can produce black traces on the radiographic film. These black traces were made by outer radiation generated by nanofibers and the radiation has to be in the X-ray region of electromagnetic spectra, because the radiation of lower energy is absorbed by the shield film. Radiographic method of X-ray detection is efficient

and sensitive. It is obvious that this method did not tell us anything about its spectrum, but it can clearly show its space distribution. The humidity, temperature and rheological parameters of polymer can affect the X-ray intensity generated by nanofibers.⁴⁵ The necessity of modeling in electrospinning and a quick outlook of some important models will be discussed as follows.

MODELING ELECTROSPINNING OF NANOFIBERS

Using theoretical prediction of the parameter effects on jet radius and morphology can significantly reduce experimental time by identifying the most likely values that will yield specific qualities prior to production.³⁵ All models start with some assumptions and have shortcomings that need to be addressed.¹⁵ The basic principles for dealing with electrified fluids that Taylor⁴⁷ discovered cannot account for the most electrical phenomena involving fluids flow under seemingly reasonable assumptions that the fluid is either a perfect dielectric or a perfect conductor. The reason is that any perfect dielectric still contains a non-zero free charge density. During steady jetting, a straight part of the jet occurs next to the Taylor cone in which only axisymmetric motion of the jet is observed. This region of the jet remains stable in time. However, further along its path, the jet can be unstable by non-axisymmetric instabilities, such as bending and branching, where lateral motion of the jet is observed in the part near the collector.¹⁰

Branching as the instability of the electrospinning jet can happen quite regularly along the jet if the electrospinning conditions are selected appropriately. Branching is a direct consequence of the presence of surface charges on the jet surface, as well as of the externally applied electric field. The bending instability leads to drastic stretching and thinning of polymer jets towards nanoscale in cross-section. Electrospun jets also create perturbations similar to undulations, which can be the source of various secondary instabilities leading to nonlinear morphologies developing on the jets.¹⁸ The bending instabilities occurring during electrospinning were studied and mathematically modeled by Reneker *et al.*⁵⁵ by viscoelastic dumbbells connected together. Both electrostatic and fluid dynamic instabilities can contribute to the basic operation of the process.¹⁹

Different stages of electrospun jets were investigated by different mathematical models by one or three dimensional techniques.^{8,56} Physical models, studying the jet profile, the stability of the jet and the cone-like surface of the jet, were developed due to significant effects of jet shape on fiber qualities.⁷ Droplet deformation, jet initiation and, in particular, the bending instability, which control, to a major extent, fiber sizes and properties, are controlled apparently predominantly by charges located within the flight jet.¹⁸ An accurate and predictive tool using a verifiable model, which accounts for multiple factors, would provide a means to run many different scenarios quickly without the cost and time of experimental trial-and-error.³⁵

An outlook to significant models

The models typically treat jet mechanics by using the localized-induction approximation by analogy to aerodynamically driven jets. The viscoelasticity of the spinning fluid and solvent evaporation in the jet were argued in most of the models. Although these models can describe the bending instability and fiber morphology, they may not accurately design and control the electrospinning process because of difficulty in measuring model variables.¹⁰ Some noteworthy models are presented below.

Leaky dielectric model

The principles for dealing with electrified fluids were summarized by Melcher and Taylor.⁴⁹ Their research showed that it is impossible to explain most of the electrical phenomena involving fluids flow given the hypothesis that the fluid is either a perfect dielectric or a perfect conductor, since both the permittivity and the conductivity affect the flow. An electrified liquid always includes free charge. Although the charge density may be small enough to ignore bulk conduction effects, the charge will accumulate at the interfaces between fluids. The presence of this interfacial charge will result in an additional interfacial stress, especially a tangential stress, which in turn will modify the fluid dynamics.^{49,57} When the conductivity is finite, the leaky dielectric model can be used.⁵⁸ Saville indicated that in the solution with weak conduction, the jet carries electric charges only on its surface.⁵⁷⁻⁵⁸ The electrohydrodynamic theory proposed by

Taylor as the leaky dielectric model is capable of predicting the drop deformation in qualitative agreement with the experimental observations.⁴⁶⁻⁴⁷

Although Taylor's leaky dielectric theory provides a good qualitative description for the deformation of a Newtonian drop in an electric field, the validity of its analytical results is strictly limited to the drop experiencing small deformation in an infinitely extended domain. Comprehensive experiments showed a serious difference from this theoretical prediction.⁴⁶ Some investigations were done to solve this defect. For example, the leaky dielectric model was modified by consideration of the charge transport to examine electro-kinetic effects.⁵⁷⁻⁵⁸

Whipping model

Whipping model is a model for the electrospinning process that mathematically depicts the interaction between the electric field and fluid properties.^{17,59} This model basically works by comparing theory with experimental data. The critical point in this model is determining an accurate treatment for understanding better the physical mechanism of charge transport near the nozzle to have a good prediction, which is not accurately conceivable especially for highly conductive fluids. By giving the shape and charge density of a jet, this model can predict both when and how the jet will become unstable.¹⁷

Although this model may be applied to predict "terminal" jet diameter, the mathematically derived limiting diameter is equated with experimentally measured fiber diameter.^{17,59}

The diameter depends only on the flow rate, electric current, and surface tension:

$$h_t = c \left(\frac{I}{Q} \right)^{-2/3} \gamma^{1/3} \quad (12)$$

where c is constant.⁶⁰

The significant assumptions in the derivation of this "terminal" diameter comprise uniform electric field. There is no phase change and no inelastic stretching of the jet. The experimental research showed that this model can be qualitatively valid for selected polymeric solutions including polyethylene oxide (PEO) and polycaprolactone (PCL) in low concentrations.^{17,59}

The simplified version of the model predicts that:

- At the early stages of whipping behavior, the amplitude of the whipping jet h is controlled by charge repulsion and inertia, and h grows exponentially with time in agreement with the earlier linear instability analysis.

- At the next stages of whipping, the inertia effects are damped by viscosity, and the envelope of the whipping jet is controlled by the interplay of charge repulsion and stretching viscosity.

- At the end of the whipping/stretching the surface tension balances the charge repulsion and sets the terminal diameter.^{17,60}

Shape evaluation model of electrospinning droplets

Knowledge of the drops' behavior in an electric field plays a critical role in practical applications. Of practical importance in the processes is electric field-driven flow.⁴⁶ The investigations on the shape evolution of small droplets attached to a conducting surface showed that it depends on the electric field intensity. Based on numerical solution of the Stokes equations for perfectly conducting droplets, different scenarios of droplet shape evolution are distinguished. For this purpose, Maxwell stresses and surface tension were investigated.^{13,61} The advantages of this model are that the non-Newtonian effect on the drop dynamics is successfully identified on the basis of electrohydrostatics. In addition, the model shows that the deformation and breakup modes of the non-Newtonian drops are distinctively different from the Newtonian cases. A restriction in this model consists in the electrohydrostatic properties of the flow, which should be highly conductive and much less viscous.⁴⁶

Non-linear model

During large-strain stretching of the polymer, non-linear viscoelasticity models must be used understanding the role of rheology.⁶² For example, a simple two-dimensional model can be used for describing the formation of barb electrospun polymer nanowires with a perturbed swollen cross-section and the electric charges "frozen" into the jet surface. This model is integrated numerically using the Kutta-Merson method with the adoptable time step. The result of this modeling is explained theoretically as a result of relatively slow charge relaxation compared to the development of the

secondary electrically driven instabilities, which deform jet surface locally. When the disparity of the slow charge relaxation, compared to the rate of growth of the secondary electrically driven instabilities, becomes even more pronounced, the barbs transform in full scale long branches. The competition between charge relaxation and rate of growth of capillary and electrically driven secondary localized perturbations of the jet surface is affected not only by the electric conductivity of polymer solutions but also by their viscoelasticity. Moreover, a nonlinear theoretical model was able to resemble the main morphological trends recorded in the experiment.¹⁸

Coupled field forces mathematical model for electrospinning process

There is not a theoretical model to describe the electrospinning process under the multi-field forces; therefore, a simple model might be very useful to indicate the contributing factors. Modeling this process can be done in two ways: a) the deterministic approach using classical mechanics like Euler approach and Lagrange approach; b) the probabilistic approach using E-infinite theory and quantum like properties. Many basic properties are harmonious by adjusting electrospinning parameters, such as voltage and flow rate, which cannot be fully explained.⁹

Slender-body model

One-dimensional models are used for inviscid, incompressible, axisymmetric, annular liquid jets under gravity. In this model, regular perturbations for slender or long jets can be expanded by using integral formulations, Taylor's series expansions, weighted residuals, and variational principles.^{36,63}

Some assumptions that applied from Feng's theory for modeling jets and drops are as follows: the jet radius decreases slowly along z direction, while the velocity is uniform in the cross-section of the jet, so it is lead to the non-uniform elongation of the jet. The parameters can be divided into three categories: process parameters (Q , I and E_∞), geometric parameters (R_0 and L) and material parameters (ρ , η_0 (the zero-shear-rate viscosity), ε , $\bar{\varepsilon}$, K , and γ). The jet can be represented by four steady-state equations: the conservation of mass and

electric charges, the linear momentum balance and Coulomb's law for the E field.

Mass conservation can be stated by:

$$\pi R^2 v = Q \quad (13)$$

R: Jet radius

The second equation in this modeling is charge conservation that can be stated by:

$$\pi R^2 KE + 2\pi R v \sigma = I \quad (14)$$

The linear momentum balance is:

$$\rho v v' = \rho g + \frac{3}{R^2} \frac{d}{dz} (\eta R^2 v) + \frac{\gamma R'}{R^2} + \frac{\sigma \sigma'}{\epsilon} + (\epsilon - \bar{\epsilon}) E E' + \frac{2\sigma E}{R} \quad (15)$$

Coulomb's law for electric field:

$$E(z) = E_\infty(z) - \ln \chi \left(\frac{1}{\epsilon} \frac{d(\sigma R)}{dz} - \frac{\beta}{2} \frac{d^2(ER^2)}{dz^2} \right) \quad (16)$$

L: The length of the gap between the nozzle and deposition point

R₀: The initial jet radius

$$\beta = \frac{\epsilon'}{\epsilon} - 1 \quad (17)$$

$$\chi = L/R_0 \quad (18)$$

By these four equations, the four unknown functions R, v, E and σ are identified.

In the first step, the characteristic scales, such as R₀ and v₀, are ranged into dimensionless groups. Inserting these dimensionless groups in the four equations discussed above, the final dimensionless equations are obtained. The boundary conditions of the four equations, which become dimensionless, can be expressed (see Figure 5) as:

$$\ln z = 0 \quad R(0) = 1 \quad \sigma(0) = 0$$

$$\ln z = \chi \quad E(\chi) = E_\infty$$

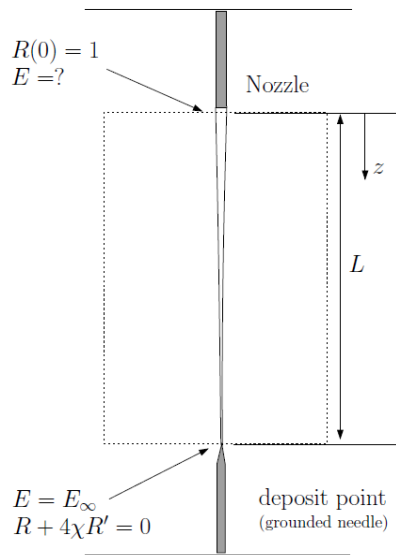


Figure 5: Boundary conditions¹

The first step is to write the ODEs as a first-order system. The basic idea is to introduce new variables, one for each variable in the original problem and one for each of its derivatives up to one less than the highest derivative appearing. In the first step, an initial guess uses for χ and the other parameters would change according to χ.^{1,64} The limitation of slender-body theory is: avoiding treating physics near the nozzle directly.³⁶

Viscoelastic fluids model for electrospinning

When the jet thins, the surface charge density varies, which in turn affects the electric field and the pulling force. Roozmond combined the “leaky dielectric model” and the “slender-body approximation” for modeling electrospinning viscoelastic jets.⁵⁴ It must be considered that all variables are uniform on the cross-section of the jet, and vary only along z.⁶² The jet could be represented by four steady-state equations: the

conservation of mass and electric charges, the linear momentum balance and Coulomb's law for the electric field, with all quantities depending only on the axial position z . The equations can be converted to dimensionless form using some characteristic scales and dimensionless groups like most of the models. These equations could be solved by converting to ODE forms and using suitable boundary conditions like slender-body model.^{36,64}

Mathematical model for AC-electrospinning

Many of the nanofiber researches reported so far have focused on nanofibers made from DC potential.⁷ In DC-electrospinning, the fiber instability or 'whipping' made it difficult to control the fiber location and the resulting microstructure of electrospun materials. To overcome these limitations, some new technologies were applied in the electrospinning process. The investigations proved that the AC potential resulted in a significant reduction in the amount of fiber 'whipping' and the resulting mats exhibited a higher degree of fiber alignment, but contained more residual solvent. In AC-electrospinning, the jet is inherently unsteady due to the AC potential unlike DC ones, so all thermal, electrical, and hydrodynamic parameters were considered to be effective in the process.⁶⁵⁻⁶⁶

The governing equations for an unsteady flow of an infinite viscous jet pulled from a capillary orifice and accelerated by an AC potential can be expressed as follows:

- 1) The conservation of mass equation;
- 2) Conservation of charge;
- 3) The Navier-Stokes equation;

$$\rho \left(\frac{\partial v}{\partial t} + v \cdot \nabla v \right) = -\nabla P + \nabla \cdot \tau + F \quad (19)$$

Using these governing equations, the final model of AC electrospinning is able to find the relationship between the radius of the jet and the axial distance from nozzle, and a scaling relation between fiber radius and the AC frequency.⁶⁶

Allometry in electrospinning

Electrospinning applies electrically generated motion to spin fibers; therefore, it is difficult to predict the size of the produced fibers, which mainly depends on the applied voltage. Therefore,

the relationship between the radius of the jet and the axial distance from the nozzle became a subject of investigation.⁶⁷ It can be described as an allometric equation by using the values of the scaling exponent for the initial steady stage, instability stage, and terminal stage.⁶⁸

The relationship between r and z can be expressed as an allometric equation of the form:

$$r \approx z^b \quad (20)$$

where b is the power exponent. When $b = 1$ the relationship is isometric and when $b \neq 1$ the relationship is allometric.^{67,69}

It is assumed that the volume flow rate (Q) and the current (I) remains unchanged during the electrospinning procedure. Many experimental data show a power law relationship between electric current and solution flow rate under the condition of fixed voltage:

$$I \approx Q^b \quad (21)$$

where b is the same as in the previous equation.⁷⁰

Due to high electrical force acting on the jet, it can be illustrated as:⁶⁷

$$\frac{d}{dz} \left(\frac{v^2}{2} \right) = \frac{2\sigma E}{\rho r} \quad (22)$$

Equations of mass and charge conservations are applied here as mentioned before.^{67,69-70}

From the above equations, it can be seen that

$$(23): \quad v \approx r^{-2}, \quad \sigma \approx r, \quad E \approx r^{-2}, \quad \frac{du^2}{dz} \approx r^{-2},$$

$$r \approx z^{-1/2}$$

Allometric scaling law

The charged jet can be considered as a one-dimensional flow, as mentioned. If the conservation equations are modified, they would be changed as:⁶⁷

$$2\pi r \sigma^\alpha v + k\pi r^2 E = I \quad (24)$$

$$r \approx z^{-\alpha/(\alpha+1)} \quad (25)$$

where α is a surface charge parameter, the value of α depends on the surface charge in the jet; when $\alpha = 0$ and 1 .⁶⁷

Multiple jet model of electrospinning

It was experimentally and numerically demonstrated that the jets from multiple nozzles show higher repulsion to other neighboring jets due to Coulombic forces than jets spun by a single

nozzle process.⁵ Yarin and Zussman⁷¹ achieved upward electrospinning of fibers from multiple jets without the use of nozzles; instead using the spiking effect of a magnetic liquid. For large-scale nanofibre production and the increase in production rate, multi-jet electrospinning systems can be designed to increase both productivity and covering area.⁷²⁻⁷³ The linear Maxwell model and non-linear Upper-Convected Maxwell (UCM) model were used to calculate the viscoelasticity. By using these models, the primary and secondary bending instabilities can be calculated. Maxwell model and the non-linear UCM model lead to rather close results in the flow dominated by the electric forces. In a multiple-nozzle set-up, not only the external applied electric field and self-induced Coulombic interactions, but also mutual-Coulombic interactions between different jets influence the jet path.⁷³

A mathematical model of the magnetic electrospinning process

Various forces that act on the polymeric jet make the jet flow whip in a circle and elongate larger and larger.⁵⁶ For controlling the instability, magnetic electrospinning is proposed. For describing the magnetic electrospun jet, Reneker's model can be used.⁵⁵ This model can not consider the coupling effects of the thermal field, electric field and magnetic field; therefore, the momentum equation for the motion of the beads is:⁷⁴

$$m \frac{d^2 r_i}{dt^2} = F_C + F_E + F_{ve} + F_B + F_q \quad (26)$$

Wan *et al.*⁷⁵ also established an electro-magnetic model to explain the bending instability of the charged jet in the electrospinning process. In order to verify the validity of the model, the motion path of the jet was then simulated numerically. The results showed that the magnetic field generated by the electric current in the charged polymer jet might be one of the main reasons which caused the helix motion of the jet during electrospinning.⁷⁵

Electrospinning nanoporous materials model

The electrospun nanoporous materials have received recently much attention due to their potential for a broad range of applications in widely different areas such as photonic structures, microfluid channels (nanofluidics), catalysis,

sensors, medicine, pharmacy and drug delivery.²⁸ Due to this importance, some theoretical models were focused on preparing electrospun nanoporous materials with controllable pore sizes and numbers.

Xu *et al.*⁷⁶ applied the following theoretical model for electrospinning dilation. In this model, the radius of the jet decreases with the increase of the velocity of the incompressible charged jet. The critical jet velocity (maximum velocity before jet changing into unstable form) is calculated as:

$$v_{cr} = Q / \pi r_{cr}^2 \quad (27)$$

where r_{cr} is radius of jet before changing into unstable form.

The velocity can exceed this critical value if a higher voltage is applied. In order to keep the conservation of mass equation, the jet dilates by decreasing its density, leading to porosity of the electrospun fibers; this phenomenon is called electrospinning-dilation.

The properties of electrospun nanoporous microspheres can be predicted using the following equation:

$$\pi r_{cr}^2 \tilde{\rho} v_0 = \pi R^2 \tilde{\rho} v_{min} = Q \quad (28)$$

where $\tilde{\rho}$ is the density of dilated microsphere, v_0 is the velocity of the charged jet at $r = r_{cr}$, R is the maximal radius of the microsphere, v_{min} is the minimal velocity. Higher voltage means higher value of the jet speed at $r = r_{cr}$, and a more drastic electrospinning-dilation process happens, resulting in a lower density of dilated microsphere, smaller size of the microsphere and smaller pores as well.^{42,76}

SUMMARY AND OUTLOOK

Electrospinning is a very simple and versatile method of creating polymer-based high-functional and high-performance nanofibers that can revolutionize the world of structural materials. The process is versatile in that there is a wide range of polymer and biopolymer solutions or melts that can spin. The electrospinning process is a fluid dynamics related problem. In order to control the property, geometry, and mass production of the nanofibers, it is necessary to understand quantitatively how the electrospinning process transforms the fluid solution through a millimeter diameter capillary tube into solid fibers, which are

four to five orders smaller in diameter. When the applied electrostatic forces overcome the fluid surface tension, the electrified fluid forms a jet out of the capillary tip towards a grounded collecting screen. Although electrospinning gives continuous nanofibers, mass production and the ability to control nanofiber properties have not been obtained yet. A combination of both theoretical and experimental approaches seems to be a promising step for a better description of the electrospinning process. Applying simple models of the process would be useful in atoning the lack of systematic, fully characterized experimental observations and the theoretical aspects in predicting and controlling effective parameters. The analysis and comparison of the model with experiments identify the critical role of the spinning fluid's parameters. The theoretical and quantitative tools developed in different models provide semi-empirical methods for predicting ideal electrospinning process or electrospun fiber properties. In each model, the researchers tried to improve the existing models or changed the tools in electrospinning by using another view. A real mathematical model, or, more accurately, a real physical model, might initiate a revolution in understanding dynamic and quantum-like phenomena in the electrospinning process. A new theory is very necessary, which would bridge the gap between Newton's world and the quantum world.

Symbols	Definition
ρ_m	Mass density
P	Pressure
t	Time
γ	Surface tension
η	Viscosity
τ	Stress tensor
ζ	Surface deflection
Q	Constant volume flow rate
v	Jet velocity
I	The current carried by the jet
K	Electrical conductivity
E	Electric field
σ	Surface charge density
ε	The dielectric constants of the jet
$\bar{\varepsilon}$	The dielectric constants of the ambient air
\mathcal{E}	The position of bead i
F_i	The net Coulomb force
F_C	The electric field force
F_E	The viscoelastic force
F_{ve}	The surface tension force

F_B	The Lorenz force
F_q	Body force
F	Terminal diameter
h_t	The dimensionless conductivity of the fluid
k	

REFERENCES

- ¹ E. T. Thostenson, C. Li and T. W. Chou, *Compos. Sci. Technol.*, **65**, 491 (2005).
- ² S. Iijima, *Nature*, **354**, 56 (1991).
- ³ D. S. Bethune, C. H. Klang, M. S. De Vries, G. Gorman, R. Savoy, J. Vazquez and R. Beyers, *Nature*, **363**, 605 (1993).
- ⁴ D. H. Reneker and I. Chun, *Nanotechnology*, **7**, 216 (1996).
- ⁵ G. Kim, Y. S. Cho and W. D. Kim, *Eur. Polym. J.*, **42**, 2031 (2006).
- ⁶ S. Karra, Mechanical Engineering 2007, Indian Institute of Technology, Madras, p. 60.
- ⁷ S. A. Theron, E. Zussman and A. L. Yarin, *Polymer*, **45**, 2017 (2004).
- ⁸ Z. Liu, Y. Jiao, Y. Wang, C. Zhou and Z. Zhang, *Adv. Drug Deliver. Rev.*, **60**, 1650 (2008).
- ⁹ L. Xu, *Chaos Soliton. Fract.*, **42**, 1463 (2009).
- ¹⁰ E. M. Helgeson, N. K. Grammatikos, M. J. Deitzel and J. N. Wagner, *Polymer*, **49**, 2924 (2008).
- ¹¹ N. Bhardwaj and S. C. Kundu, *Biotechnol. Adv.*, **28**, 325 (2010).
- ¹² M. Bognitzki, W. Czado, T. Frese, A. Schaper, M. Hellwig *et al.*, *Adv. Mater.*, **13**, 70 (2001).
- ¹³ O. A. Basaran and R. Suryo, *Nat. Phys.*, **3**, 679 (2007).
- ¹⁴ V. Mottaghitalab and A. K. Haghi, *Korean J. Chem. Eng.*, **28**, 114 (2011).
- ¹⁵ N. Titchenal and W. Schrepple, *Mater. Sci. Eng.*, **460**, 1 (2002).
- ¹⁶ Y. M. Shin, M. M. Hohman, M. P. Bernner and G. C. Rutledge, *Polymer*, **42**, 9955 (2001).
- ¹⁷ M. Hohman, M. Shin, G. Rutledge and M. P. Brenner, *Phys. Fluid.*, **13**, 2201 (2001).
- ¹⁸ A. Holzmeister, A. L. Yarin and J. H. Wendorff, *Polymer*, **51**, 2769 (2010).
- ¹⁹ A. Frenot and I. S. Chronakis, *Curr. Opin. Colloid Interface Sci.*, **8**, 64 (2003).
- ²⁰ I. Y. Kim, S. J. Seo, H. S. Moon, M. K. Yoo, I. Y. Park *et al.*, *Biotechnol. Adv.*, **26**, 1 (2008).
- ²¹ D. Czaplewski, J. Kameoka and H. G. Craighead, *J. Vac. Sci. Technol. B*, **21**, 2994 (2003).
- ²² M. Ziabari, V. Mottaghitalab and A. K. Haghi, *Korean J. Chem. Eng.*, **25**, 905 (2008).
- ²³ M. Ziabari, V. Mottaghitalab, S. T. McGovern and A. K. Haghi, *Nanoscale Res. Lett.*, **2**, 597 (2007).

- ²⁴ S. Abdul Karim, A. Sulong, C. Azhari, T. Lee and N. Hwei, *J. Appl. Sci. Res.*, **8**, 2510 (2012).
- ²⁵ K. Nasouri, H. Bahrambeygi, A. Rabbi, A. Mousavi Shoushtari and A. Kafrou, *J. Appl. Polym. Sci.*, **126**, 127 (2012).
- ²⁶ R. Faridi-Majidi, H. Ziyadi, N. Naderi and A. Amani, *J. Appl. Polym. Sci.*, **124**, 1589 (2012).
- ²⁷ A. Rabbi, K. Nasouri, H. Bahrambeygi, A. Mousavi Shoushtari and M. Babaei, *Fibers Polym.*, **13**, 1007 (2012).
- ²⁸ M. Ziabari, V. Mottaghitlab and A. K. Haghi, *Korean J. Chem. Eng.*, **25**, 923 (2008).
- ²⁹ H. Fong, I. Chun and D. H. Reneker, *Polymer*, **40**, 4585 (1999).
- ³⁰ J. H. Yu, S. V. Fridrikh and G. C. Rutledge, *Polymer*, **47**, 4789 (2006).
- ³¹ K. M. Forward and G. C. Rutledge, *Chem. Eng. J.*, **183**, 492 (2012).
- ³² T. A. Kowalewski, S. Blonski and S. Barral, *Bull. Pol. Acad. Sci. Tech. Sci.*, **53**, 385 (2005).
- ³³ M. Ziabari, V. Mottaghitlab and A. K. Haghi, *Korean J. Chem. Eng.*, **27**, 340 (2010).
- ³⁴ M. Trojanowicz, *TrAC Trends Anal. Chem.*, **25**, 480 (2006).
- ³⁵ C. J. Thompson, G. G. Chase, A. L. Yarin and D. H. Reneker, *Polymer*, **48**, 6913 (2007).
- ³⁶ J. J. Feng, *Phys. Fluid.*, **14**, 3912 (2002).
- ³⁷ M. E. Helgeson and N. J. Wagner, *AIChE*, **53**, 51 (2007).
- ³⁸ A. Doustgani, E. Vasheghani-Farahani, M. Soleimani and S. Hashemi-Najafabadi, *Compos. Part B Eng.*, **43**, 1830 (2012).
- ³⁹ S. V. Fridrikh, J. H. Yu, M. P. Brenner and G. C. Rutledge, *Phys. Rev. Lett.*, **90**, 144502 (2003).
- ⁴⁰ G. C. Rutledge and S. V. Fridrikh, *Adv. Drug Deliver. Rev.*, **59**, 1384 (2007).
- ⁴¹ A. Thess, R. Lee, P. Nikolaev, H. Dai, P. Petit *et al.*, *Science*, **273**, 483 (1996).
- ⁴² J. H. He, L. Xu, Y. Wu and Y. Liu, *Polym. Int.*, **56**, 1323 (2007).
- ⁴³ H. K. Rasmussen and O. Hassager, *J. Non-Newton. Fluid Mech.*, **46**, 298 (1993).
- ⁴⁴ M. Wang, J. He, J. Yu and N. Pan, *Int. J. Therm. Sci.*, **46**, 848 (2007).
- ⁴⁵ Z. K. Tang, L. Zhang, N. Wang, X. X. Zhang, G. H. Wen *et al.*, *Science*, **292**, 2462 (2001).
- ⁴⁶ J. W. Ha and S. M. Yang, *J. Fluid Mech.*, **405**, 131 (2000).
- ⁴⁷ G. I. Taylor, *Procs. R. Soc. Lond. A. Math. Phys. Sci.*, **291**, 159 (1966).
- ⁴⁸ Y. Q. Wan, Q. Guo and N. Pan, *Int. J. Nonlinear Sci. Num. Simul.*, **5**, 5 (2004).
- ⁴⁹ J. R. Melcher and G. I. Taylor, *Annu. Rev. Fluid Mech.*, **1**, 111 (1969).
- ⁵⁰ A. L. Yarin, S. Koombhongse and D. H. Reneker, *J. Appl. Phys.*, **89**, 3018 (2001).
- ⁵¹ P. R. de Souza Mendes, *J. Non-Newton. Fluid Mech.*, **147**, 109 (2007).
- ⁵² P. Pokorný, P. Mikes and D. Lukáš, *Europhys. Lett.*, **92**, 47002 (2010).
- ⁵³ C. P. Firme and R. B. Prabhakar, *Nanomed. Nanotechnol. Biol. Med.*, **6**, 245 (2010).
- ⁵⁴ K. G. Kornev, *J. Appl. Phys.*, **110**, 124910 (2011).
- ⁵⁵ D. H. Reneker, A. L. Yarin, H. Fong and S. Koombhongse, *J. Appl. Phys.*, **87**, 4531 (2000).
- ⁵⁶ J. H. He, Y. Q. Wan and L. Xu, *Chaos Soliton. Fract.*, **33**, 26 (2007).
- ⁵⁷ D. A. Saville, *Annu. Rev. Fluid Mech.*, **29**, 27 (1997).
- ⁵⁸ D. T. Parageorgiou and J. M. V. Broeck, *IMA J. Appl. Math.*, **72**, 832 (2007).
- ⁵⁹ K. Sarkar, M. B. Ghaliya, Z. Wu and S. C. Bose, *J. Mater. Process. Technol.*, **209**, 3156 (2009).
- ⁶⁰ H. Touhara, A. Yonemoto, K. Yamamoto, S. Komiyama, S. Kawasaki *et al.*, *J. Fluorine Chem.*, **114**, 181 (2002).
- ⁶¹ S. N. Reznik, A. L. Yarin, A. Theron and E. Zussman, *J. Fluid Mech.*, **516**, 349 (2004).
- ⁶² J. J. Feng, *J. Non-Newton. Fluid Mech.*, **116**, 55 (2003).
- ⁶³ J. I. Ramos, *Appl. Math. Model.*, **20**, 593 (1996).
- ⁶⁴ C. Wang, Z. X. Guo, S. Fu, W. Wu and D. Zhu, *Prog. Polym. Sci.*, **29**, 1079 (2004).
- ⁶⁵ Y. M. Shin, M. M. Hohman, M. P. Brenner and G. C. Rutledge, *Appl. Phys. Lett.*, **78**, 3 (2001).
- ⁶⁶ H. Ji-Huan, W. Yue and P. Ning, *Int. J. Nonlinear Sci. Num. Simul.*, **6**, 243 (2005).
- ⁶⁷ J. H. He and H. M. Liu, *Nonlinear Anal.*, **63**, 919 (2005).
- ⁶⁸ J. H. He, Y. Q. Wan and J. Y. Yu, *Int. J. Nonlinear Sci. Num. Simul.*, **5**, 243 (2004).
- ⁶⁹ J. H. He and Y. Q. Wan, *Polymer*, **45**, 6731 (2004).
- ⁷⁰ J. H. He, Y. Q. Wan and J. Y. Yu, *Polymer*, **46**, 2799 (2005).
- ⁷¹ A. L. Yarin and E. Zussman, *Polymer*, **45**, 2977 (2004).
- ⁷² A. Varesano, R. A. Carletto and G. Mazzuchetti, *J. Mater. Process. Technol.*, **209**, 5178 (2009).
- ⁷³ S. A. Theron, A. L. Yarin, E. Zussman and E. Kroll, *Polymer*, **46**, 2889 (2005).
- ⁷⁴ L. Xu, Y. Wu and Y. Nawaz, *Comput. Math. Appl.*, **61**, 2116 (2011).
- ⁷⁵ S. Wan, G. Wei-Jie, L. Yong, Y. Bin and Y. Gui-Sheng, *Adv. Sci. Lett.*, **10**, 566 (2012).
- ⁷⁶ L. Xu, F. Liu and N. Faraz, *Comput. Math. Appl.*, **64**, 1017 (2012).